SECURITY CLASSIFICATION OF THIS PAGE (When Data Entered)

REPORT DOCUMENTATION PAGE

READ INSTRUCTIONS
BEFORE COMPLETING FORM

1. REPORT NUMBER	2. GOVT ACCESSION NO.	3. RECIPIENT'S CATALOG NUMBER

4. TITLE (and Subtitle)	5. TYPE OF REPORT & PERIOD COVERED
Wave power extraction by floating bodies	Technical Report
	6. PERFORMING ORG. REPORT NUMBER

7. AUTHOR(s)	8. CONTRACT OR GRANT NUMBER(s)
C.C. Mei and J.N. Newman	N00014-76-C-0214

9. PERFORMING ORGANIZATION NAME AND ADDRESS	10. PROGRAM ELEMENT, PROJECT, TASK AREA & WORK UNIT NUMBERS
R.M. Parsons Laboratory, Dept. of Civil Engrg. Massachusetts Institute of Technology Cambridge, MA 02139	NR 062-228

11. CONTROLLING OFFICE NAME AND ADDRESS	12. REPORT DATE
Office of Naval Research	November 1979
	13. NUMBER OF PAGES
	28

14. MONITORING AGENCY NAME & ADDRESS(if different from Controlling Office)	15. SECURITY CLASS. (of this report)
	15a. DECLASSIFICATION/DOWNGRADING SCHEDULE

16. DISTRIBUTION STATEMENT (of this Report)

Material unclassified; distribution unlimited.

17. DISTRIBUTION STATEMENT (of the abstract entered in Block 20, if different from Report)

DDC
RECEIVED
DEC 12 1979
A

18. SUPPLEMENTARY NOTES

19. KEY WORDS (Continue on reverse side if necessary and identify by block number)

20. ABSTRACT (Continue on reverse side if necessary and identify by block number)

The linearized theory of water waves is reviewed in the context of wave-energy absorbers. A global analysis is outlined, leading to relative simple expressions for the maximum energy absorption. Calculations are presented for the performance of a Salter cam in two dimensions, and of a Cockerell raft in both two and three dimensions. Similar rates of optimum energy absorption are anticipated for other devices including the Kaimei ship and French air bag.

DD FORM 1473 EDITION OF 1 NOV 65 IS OBSOLETE
1 JAN 73
S/N 0102-LF-014-6601

SECURITY CLASSIFICATION OF THIS PAGE (When Data Entered)

WAVE POWER EXTRACTION BY FLOATING BODIES

C.C. Mei   J.N. Newman

Department of Civil Engineering   Department of Ocean Engineering

Massachusetts Institute of Technology

Cambridge, Mass. 02139, U.S.A.

ABSTRACT

   The linearized theory of water waves is reviewed in the context of wave-energy absorbers. A global analysis is outlined, leading to relatively simple expressions for the maximum energy absorption. Calculations are presented for the performance of a Salter cam in two dimensions, and of a Cockerell raft in both two and three dimensions. Similar rates of optimum energy absorption are anticipated for other devices including the Kaimei ship and French air bag.

1. INTRODUCTION

The conversion of wave energy from the ocean is an important and contemporary field of application for the theoretical methods which have been utilized in ship hydrodynamics and other related fields. Since there is no extensive base of empirical design information for wave-power devices, theoretical methods are especially useful in this field.

The basic theory for analyzing wave-body interactions is well developed, under the usual assumptions of small oscillatory motions and neglect of viscous effects. This approach has been pursued extensively in the field of ship hydrodynamics (Wehausen, 1971; Newman, 1978). The necessary generalizations to analyze various wave-energy devices require trivial extensions from six degrees of rigid-body motion to account for the pertinent "higher-order modes" such as the relative angular displacement at the hinge of a Cockerell raft, or the oscillatory displacement of the internal free surface in a National Engineering Laboratory device.

The classic theory for wave-body interactions is based upon the use of a linearized velocity potential. The overall problem can be decomposed into linear components including the incident wave system, the scattering disturbance of the incident wave by the stationary body, and the radiation disturbances due to each mode of body motion. For a given body geometry the scattered and radiation potentials may be derived by a variety of techniques, generally involving numerical analysis (Mei, 1978).

In the direct approach each of these potentials is found and the corresponding components of the pressure follow from Bernoulli's equation. The hydrodynamic forces are determined directly by integration over the wetted surface of the vessel. (The term "force" is used here in a generalized sense, to include the moment and any pertinent higher-order loads.) Equations of motion follow for the various degrees of freedom of the vessel, and it is straightforward to solve for the unsteady motions and for the rate of energy absorption.

An alternative global analysis can be based in part on the principle of energy conservation, and more generally on the application of Green's theorem to the various separate components of the velocity potential. This approach is useful particularly to determine the optimum power output from a given configuration. In this way it is possible to determine the maximum output, as a rational design goal, and to avoid the limitations of performance and lengthy experiments which result from a purely

2

intuitive design approach.

The global analysis provides a relatively simple prediction of the power absorption, and other characteristics of the device, including the wave damping and exciting forces, in terms of the far-field asymptotic form of the radiation potentials. However, the added-mass force in quadrature with the body velocity must be determined from a direct local solution of the radiation potential. Thus a direct solution of the radiation problem is required, for each pertinent degree of freedom, to provide a complete description of the relevant hydrodynamic characteristics of the device.

The theory is simplified if the fluid motion is two-dimensional, implying a long cylindrical device with its axis parallel to the wave crests. The resulting analysis has given much inspiration to this field, but practical considerations suggest that alternative configurations with smaller transverse dimensions may be more economical, especially in respect to structural costs and mooring forces.

This paper is intended to review the basic theoretical approach to wave-power devices, and to present a variety of results for specific configurations which have attracted the authors' attention. The essential elements of the theory are outlined in Section 2, with principal emphasis on the rate of energy absorption. Numerical results for specific two- and three-dimensional configurations are presented in Sections 3 to 5. In Section 6 we discuss the pertinent hydrodynamic characteristics of different types of wave-power devices.

2.   GLOBAL ANALYSIS

With the fundamental assumption of small oscillatory motions, the incident wave spectrum can be decomposed into separate sinusoidal components of prescribed frequency and direction. Therefore, it is relevant to consider the absorption of a single regular plane progressive wave system, the direction of which is taken for convenience to coincide with the horizontal x-axis. The absorbing vessel may be oriented in an arbitrary manner, but to simplify our discussion only the case of "head-seas" is considered.

Deep water is assumed, and the velocity potential of the incident waves is given by the expression

$$\phi_I = -i(gA/\omega) \exp(kz + ikx) \tag{2.1}$$

The time factor $e^{-i\omega t}$ is implied, and the real part of the resulting product is to be taken. The parameter A denotes the wave amplitude, g the gravitational acceleration, $k = \omega^2/g$ is the wavenumber, and z is the vertical coordinate.

The absorbing device is assumed to be a floating or submerged vessel, which may be rigid or flexible. Its motions may be defined by six rigid-body degrees of freedom, with complex velocities v_j, and a sequence of higher-order "flexible" motions which can be defined by extension of the same notation for j > 6. Since the solution is linearized, superposition of separate components is valid and the general expression for the velocity potential takes the form

$$\phi = \phi_I + \phi_s + \Sigma \, v_j \phi_j \tag{2.2}$$

Here ϕ_s is the scattered potential, due to the disturbance of the incident waves by the stationary vessel. The remaining components ϕ_j are due to the various degrees of freedom of its motion. In (2.2) and hereafter, summation is over all nonzero modes of motion.

Each component of (2.2) is governed by Laplace's equation, subject to linearized boundary conditions on the free surface and on the wetted surface S of the vessel. With the exception of the incident wave potential ϕ_I, each component of (2.2) also satisfies a radiation condition of outgoing waves at large distance from the vessel, such that for large values of $R = (x^2 + y^2)$,

$$\phi_j = ie^{-i\pi/4}(2\pi kR)^{-1/2} H_j(\theta) e^{ikR} , \qquad (j = s,1,2,\dots) \tag{2.3}$$

Here

$$H_j(\theta) = -k \iint_S (\frac{\partial \phi_j}{\partial n} - \phi_j \frac{\partial}{\partial n})\{\exp[kz-ik(x \cos \theta + y \sin \theta)]\}dS \tag{2.4}$$

S-body surface

is the so-called Kochin function, proportional to the amplitude of the far-field radiated waves associated with the potential ϕ_j.

From the linearized Bernoulli equation, the pressure field of the fluid, and thus the hydrodynamic forces acting upon the vessel, can be expressed in a similar form to (2.2). The total force in the i-th direction due to $\phi_I + \phi_s$ is the exciting force due to the incident wave system,

$$i\omega\rho \iint\limits_{S} (\phi_I + \phi_s) \frac{\partial\phi_i}{\partial n} dS \equiv A X_i \qquad (2.5)$$

Similarly, the force due to ϕ_i is expressed in the form

$$i\omega\rho \iint\limits_{S} \phi_j \frac{\partial\phi_j}{\partial n} dS = B_{ij} - i\omega M_{ij} \qquad (2.6)$$

where the real coefficients B_{ij} and M_{ij} are known as the damping and added mass, respectively. The damping coefficients are especially important in the context of wave power; as the components of the hydrodynamic force in phase with the velocity of the vessel; these are responsible for the radiated wave energy due to the vessel's own motions in calm water.

A direct analysis of wave power absorption requires solutions for the scattered potential and each of the "forced motion" potentials in calm water, following which the pressure force acting in each case can be found from integration. It is clear however from the "principle of virtual work" that the power absorbed will depend only on the hydrodynamic force coefficients (2.5) and (2.6), and the mechanical device restraining the body motions.

Instead of solving all the boundary value problems, much information may be obtained by using certain global relations which follow mathematically from Green's theorem. These are examined in a systematic manner by Newman (1976). The most important results, in the context of wave-power absorption, are relations for the exciting force, damping coefficients, and absorbed power, in terms of the Kochin functions, as summarized below:

The Haskind relations express the exciting force in the form

$$X_j = - \frac{i\rho g A}{k} H_j(\pi) \qquad (2.7)$$

Here X_j is the complex amplitude of the exciting force in waves, of unit amplitude, with $j = 1,2,3$ for each component of the force, $j = 4,5,6$ for the moment. Higher-order mode shapes and exciting forces can be defined similarly. The principal advantage of (2.7) is to permit the determination of the exciting force in waves without solution of the boundary value problem for the scattered potential ϕ_s.

The damping coefficients are related more directly to the outgoing radiated waves by the principle of energy conservation. Mathematically

this relationship takes the form

$$B_{ij} = \frac{\omega\rho}{4\pi k} \int_0^{2\pi} H_j(\theta) \, H_j^*(\theta) \, d\theta \tag{2.8}$$

where B_{ij} denotes the damping coefficient for the force or moment in the direction i, due to a body motion in mode j. The matrices B_{ij} and M_{ij} are symmetric.

For any combination of body modes such that the phase of the motion is constant over the body surface, in each mode, with complex amplitude v_j, the rate of energy absorbed by the body can be expressed in the form

$$\frac{\overline{dE}}{dt} = -\frac{\rho g A}{2k} \, \text{Im}[\Sigma \, v_j H_j^*(\pi)] - \frac{\omega\rho}{8\pi k} \int_0^{2\pi} \left| \Sigma \, v_j H_j(\theta) \right|^2 d\theta \tag{2.9}$$

The last expression can be interpreted physically by combining it with (2.7) and (2.8) to give

$$\frac{\overline{dE}}{dt} = \frac{1}{2} A \, \text{Re}[\Sigma \, v_j \, X_j^*] - \frac{1}{2} \Sigma\Sigma \, v_i \, X_j^* \, B_{ij} \tag{2.10}$$

This expression is equivalent to equation (4.1) of Evans (1979), where a matrix notation is used and the derivation is based on an analysis of the work done in opposition to the hydrodynamic forces on the body. Evans' derivation is for a system of N bodies, each having a single degree of freedom, but there is in principle no difference between that case and the present one, of a single body with several degrees of freedom. Indeed, the generalization to, say, N bodies with M degrees of freedom simply requires a suitable set of additional subscripts, with no other change to the analysis.

The above equations are valid in general for a three-dimensional vessel. In the special case of two-dimensional motions, resulting from the interaction of a long cylindrical vessel with its axis parallel to the wave crests, equations (2.1), (2.2) and (2.8) remain valid, but the intermediate equations are modified as noted by Newman (1976).

The equivalent expressions (2.9) and (2.10) can be used to determine the performance of a wave-absorbing device simply in terms of its respective Kochin functions, or in terms of its damping coefficients and exciting forces. The second term in (2.9) or (2.10) is a negative quantity, associated physically with outgoing energy flux due to the vessel's own wave generation. The first term in these expressions may

6

be of either sign, depending on the relative phase between the velocity component v_j and corresponding Kochin function or exciting force. Optimum performance follows by choosing the velocity components in a suitable manner.

If there is only one degree of freedom, the energy absorption is maximized by choosing the phase of this velocity to be the same as tne exciting force, and the resulting quadratic function attains a maximum value when

$$\left|v_j\right| = \frac{2\pi gA}{\omega} \frac{\left|H_j^*(\pi)\right|}{\int_0^{2\pi} \left|H_j(\theta)\right|^2 d\theta} = \frac{A\left|X_j^*\right|}{2B_{ji}} \tag{2.11}$$

It can be shown (cf. Mei, 1976) that this situation is realized if the vessel is restrained by a linear device tuned for resonance in such a manner that the inertial and restoring terms cancel, and with a mechanical damping precisely equal to the hydrodynamic damping.

Corresponding to (2.11), the maximum power absorption is given by

$$\frac{\overline{dE}}{dt} = \frac{\pi \rho g^2 A^2}{2\omega k} \frac{\left|H_j^*(\pi)\right|^2}{\int_0^{2\pi} \left|H_j(\theta)\right|^2 d\theta} \tag{2.12}$$

In this form it is apparent that an efficient wave absorbing device is one which radiates waves primarily in the direction opposite to the wave incidence or, equivalently, a vessel which experiences a relatively large exciting force in waves from this particular direction. In other words, a geometrically efficient three-dimensional wave absorber should be such that it can generate highly focused waves by its own motions.

The two-dimensional analog of (2.12) is noted by Mei (1976) and Evans (1976), and is essentially the mathematical basis for the superior performance of unidirectional wavemakers as wave absorbing devices. In particular the optimum efficiency which is attainable with one degree of freedom is

$$\varepsilon_{opt} = (1 + \left|A_+/A_-\right|^2)^{-1} \tag{2.13}$$

where A_+ and A_- are the radiated wave amplitudes towards $x \sim +\infty$ and $-\infty$, respectively, the incident wave being from $x \sim -\infty$. In this context the efficiency is defined as the ratio of the power absorbed by the device and the rate of energy flux $\frac{1}{4} \rho g^2 A^2/\omega$ per unit width of the incident

wave system.

The results for a single degree of freedom can be extended to a pair of modes of motion which are even and odd with respect to the x-axis, for example heave and surge in the case of rigid-body motions. The corresponding Kochin functions are even and odd in θ, and these do not interact in (2.9). Equivalently, in terms of (2.10), there is no cross-coupling between such modes and $B_{ij} = 0$ for $i = j$. It follows that the total energy absorption is the linear superposition of that in each separate mode.

The three-dimensional results may be illustrated by considering an axisymmetric vessel. Heave motions are independent of θ, and from the first form of (2.12) it follows that the maximum energy absorption is $\rho g^2 A^2/4\omega k$. Dividing by the rate of energy flux per unit width of wave crest in the incident waves gives a "capture width" $W = 1/k$, or approximately one sixth of the wavelength. Alternatively, surge or pitch of the same vessel gives a Kochin function proportional to $\cos \theta$, and $W = 2/k$. Superposition of these two modes gives a maximum capture width from rigid-body motions of $3/k$. Larger amounts of energy can be captured, in principle, by higher-order modes proportional to $\cos n\theta$. In all cases the optimum combination of an even and odd mode shape is related in precisely the manner to cancel the radiated waves downstream, $(\theta = 0)$ and reinforce the separate components upstream $(\theta = \pi)$.

Optimum performance of a wave-absorbing device requires that each mode is optimized in magnitude and phase. Equivalently, each mode must be restrained by a force of optimum magnitude and phase. Thus the restraint which extracts the output power must have an optimum complex impedance including inertial and dissipative components. This optimum impedance is a function of the incident wave frequency or wavelength. A simple mechanical device with constant inertia cannot satisfy this requirement for all wavelengths. The global analysis can be used in non-optimum conditions to express the rate of energy absorption to the body motions, but the latter must be computed by direct solution of the equations of motion.

3. SALTER'S CAM

Salter's cam is the first device which aroused serious interest in wave power by its remarkably high efficiency unimagined and unattained

8

heretofore. In the idealized laboratory setting, it is a long cam which can roll about a horizontal shaft parallel to the incident wave crests. As is evident from (2.13) the highest efficiency is attained when the cam radiates the most wave energy towards the incident waves. For the geometry of the early laboratory model of Salter, (2.13) has been evaluated by numerical solution of the radiation problem; the results are shown in Figure 1.

The optimum theoretical efficiency ε_{opt} varies from 0.5 at long wavelengths to 1 at short wavelengths. This variation may be understood with the help of (2.4). For long wavelengths, the Kochin function is dominated by the contribution from the term $\partial\phi_j/\partial n$ in the integrand. Thus the motion of the cam is represented effectively by a source whose strength is proportional to the change of the displaced volume. Since the waves radiated by a source are symmetrical, $A_+ = A_-$, and (2.13) then gives $\varepsilon_{opt} = 0.5$. On the other hand, at high frequencies the waves are essentially created by the left side of the cam near the free surface. For short wavelengths these waves cannot easily pass under the cam and must radiate entirely towards $x \sim -\infty$. Therefore $A_+/A_- \ll 1$ and $\varepsilon_{opt} \simeq 1$ from (2.13). The calculations show that for a wave period in the range of 8 to 15 seconds, the radius should be in the range of $4 \sim 14$ m to assure high optimum efficiency.

If the complex impedance of the restraining moment (i.e., the inertia of the cam and the extraction rates) is chosen to give ε_{opt} for a particular design frequency, then the system is not optimal for other frequencies as noted at the end of Section 2. The attainable ε falls below the curve for ε_{opt}, as is illustrated in Figure 1, where the optimum is reached at $\omega\sqrt{a/g} = 0.7$ with $\hat{\lambda}'_{33} = 1.10$. It is a positive attribute of Salter's cam that the efficiency curve is quite broad-banded. For the same cam inertia the effect of either increasing or decreasing the extraction rate $\hat{\lambda}'_{33}$ reduces the peak efficiency. However, the efficiency curve becomes flatter if $\hat{\lambda}'_{33} > 1.10$ which may be a useful property. Lastly, if the cam size is sufficiently small and the inertia large, the optimum dimensionless frequency is low. Not only is ε_{opt} drastically reduced, but the frequency band width of the ε-curve is also reduced. Thus, Salter's cam must be sufficiently large.

In Figure 2 we show the horizontal wave force on the cam. The order of magnitude of the force is, in physical terms, $\rho g a A$, which can be anticipated by using the linearized Bernoulli equation for the hydrodynamic

pressure. This implies a very large force; e.g., for a = 10 m, A = 3m, $\rho gaA \cong 30$ Tn/m. It is interesting that for extraction rates below optimum the peak force and the peak efficiency do not occur at precisely the same frequency. Mynett et al. (1979) also performed calculations for various submergence and water depths, and found the latter to have relatively little effect.

In reality a rigid shaft would demand a massive support which of course implies a high cost. A flexible support would normally lead to a loss in efficiency. Calculations based on a simple model in which the cam may slide on a vertical sleeve which may move freely horizontally show that the efficiency is usually reduced drastically, with similar reduction in wave forces. This is illustrated in Figure 3. In principle, mechanisms can be added in the cam so that energy may be extracted from all degrees of freedom to increase the efficiency, but intricate designs would be necessary which raise new technological and economical considerations. Once the details of the mechanisms are specified, computations similar to those given here are also possible.

If the wind-generated wave is assumed to be a stationary random process the averaged power flux per unit length of the crest may be related to the energy spectrum by

$$\langle P_w \rangle = \rho g \int_0^\infty S_I(\omega) C_g(\omega) d\omega \qquad (3.1)$$

while the power extracted by the rolling cam is

$$\langle P \rangle = \lambda'_{33} \langle \overset{\circ}{\alpha}{}_3^2 \rangle = \lambda'_{33} \int_0^\infty \omega^2 S_I(\omega) |\alpha_3|^2 d\omega \qquad (3.2)$$

where $\alpha_3(\omega)$ is the complex frequency response of the roll amplitude. The mean squares of the roll amplitude and of the hydrodynamic force on the shaft can also be obtained from the incident wave spectrum and the frequency response:

$$\langle \alpha_3^2 \rangle = \int_0^\infty S_I(\omega) |\alpha_3|^2 d\omega \qquad (3.3)$$

$$\langle f_1^2 \rangle = \int_0^\infty S_I(\omega) |f_1|^2 d\omega \qquad (3.4)$$

Serman and Mei (1979) have computed these mean squares based on the frequency responses of Mynett et al. (1979).

10

As wave power devices will likely be installed near the coastline, a representative JONSWAP spectrum is chosen for S_I. The spectrum is characterized by the wind speed U and the fetch length X from which various parameters, in particular the peak frequency and root mean square of the incident wave height, may be determined by empirical formulas (see Hasselmann et al., 1973). From JONSWAP spectrum the increase of root-mean-square wave height and peak period with both U and X may be calculated. The following numerical results for a cam with radius $a = 5$ m are due to Serman and are similar to those given in Serman and Mei (for $a = 3$ m). The extracted power in kw/m of course increases with both U and X as shown in Figure 4. When U and X increase, the peak frequency decreases, hence the efficiency also decreases (Figure 5); this is consistent with the ε_{opt} curve in Figure 1. Root-mean-square horizontal and vertical forces are shown in Figures 6 and 7. The root-mean-square of the angular displacement is shown in Figure 8. For example, let $X = 200$ Km, $U = 3 \sim 14$ m/sec, $<P> = 2 \sim 46$ kw/m, $F_x = 1 \sim 10$ Tn/m. It should be remarked that for these ranges of X and U the wave height is $2 \sim 4$ m so that linear approximation is still useable.

Serman and Mei (1979) also studied the performance in a Pierson-Moskowitz spectrum of a cam whose shaft can move passively in both the vertical and horizontal directions. Details are omitted here.

4. TWO-DIMENSIONAL FLOATING RAFTS

The elongated and shallow rafts of Cockerell[*], which extract energy from the relative rotation about the hinges, have the obvious advantage of smaller mooring forces. It was therefore felt desirable to provide a theoretical model for its performance. For analytical simplicity Haren and Mei (1979) studied the case of two-dimensional rafts on a sea of small depth. Because they were also interested in optimum raft lengths, computations based on the fully two-dimensional theory for arbitrary wavelength would be quite tedious. Therefore a linearized shallow water theory was used. It is interesting, however, that for a sample geometry the difference between these two theories was also found later to be not large for a wide range of frequencies. Again according to (2.12)

---

[*] Essentially the same idea has been proposed by Glen Hagen of Louisiana, U.S.A., in a patent application (No. 4077213, Official Gazette, U.S. Patent and Trademark Office, March 7, 1978, filed Feb. 13, 1976). The elongated feature was stressed more by Hagen than by Cockerell.

optimum efficiency is attained if most of the radiated waves are towards $x \sim -\infty$ and very little towards $x \sim +\infty$. This is possible if the rafts on the transmission side are much longer than the rafts on the incidence side. For the simplest case of a short raft hinged onto a fixed semi-infinite raft (which has the same effect as a fixed wall), it can be easily shown that 100% efficiency is possible if the short raft is resonated and the extraction rate equals the roll damping rate of the short raft. With only a buoyancy restoring force the corresponding raft length is 40% of the wavelength. The efficiency curve is again quite broad-banded. For a finite total length without rigid external constraint, some efficiency is expected to be lost. Experimenting with three, four and five rafts, Haren and Mei sought the optimal design under various criteria. The optimizing parameters are raft lengths and extraction rates at the hinges. The criteria include the best efficiency at a fixed total length, while the incident waves may be regular or have a smooth spectrum with one or two peaks.

For example, for a depth of 9.15 m, a regular wave of period T_p = 5.52 sec, wavelength = 52 m, total length = 137 m, the best efficiency is achieved when the three rafts are 16.8, 52, 68.3 m long and the extraction rates at the first two hinges are nearly equal to 5380 kg/m^2. The total amount of energy extracted at the first hinge exceeds 95% of the total. The efficiency for other frequencies is given in Figure 9. It may be concluded that the relative motion about the second hinge is quite small so that the system behaves like a two-raft system. Since the entire system is floating, the forces on the hinges are not large; a typical vertical force is:

$F_z \sim 0.6 \, \rho gAH = 18$ Tn/m at resonance, for A = 3 m,

which is somewhat less than that experienced by a Salter cam on a fixed axis. In practice, it may be easier to have a strong hinge between two moving rafts than to have a strong anchor to the sea bottom.

Finally in many coastal waters the presence of swell introduces two spectral peaks. The results of optimization with some consideration of cost is rather interesting. It may be shown that the profit index is $<eff> - QL_T$ where Q is proportional to the unit cost of the raft and inversely proportional to the price of electricity and the local wave energy. Sample calculations for the Northwest Pacific coast of the U.S. show that the efficiency curve follows the short wave spectral peak as shown in Figure 10, suggesting that it is cost-effective to disregard

the long wave peak. Naturally a larger Q can lead to negative profit.

5.   ELONGATED SLENDER VESSELS

The final numerical example to be presented is that of a three-dimensional Cockerell raft which is elongated in the direction perpendicular to the wave crests. More details are given by Newman (1979). A similar analysis and conclusions should apply to other devices including the Kaimei ship and French air bag.

We consider a body which is elongated in the x-direction, and subject to a vertical displacement V(x) along its depth. This motion may be expressed conveniently in terms of a sequence of modal functions, in the form

$$V(x) = \Sigma \, v_j \, f_j(x) \qquad\qquad (5.1)$$

where v_j is a complex constant. For a slender body with small beam and draft, compared to the wavelength, the Kochin function (2.4) can be approximated in a consistent manner by neglecting the second term in parenthesis.[*] For each of the above modes, it follows that

$$H_j(\theta) \cong -k \int_{-\ell/2}^{\ell/2} f_j(x) \exp(ikx \cos\theta) \, b(x) dx \qquad (5.2)$$

where ℓ is the body length and b(x) is the local waterplane beam.

For each mode j, the maximum rate of energy absorption can be determined by substituting (5.2) in (2.12). In the following examples the local beam b is assumed constant, corresponding to a vessel with rectangular waterplane. The rate of energy absorption is expressed as the product of the rate of energy flux, per unit of incident wave front, and the capture width W of the vessel.

From the computational standpoint, the Legendre polynomial $P_j(x)$ is a convenient choice of mode shape. The Kochin functions (5.2) are given in terms of spherical Bessel functions. Moreover, the modes j = 0,1 correspond respectively to rigid-body motions in heave and pitch, while

_____
[*] This approximation is essentially identical to that employed by Evans (1979) to study the interaction between several adjacent vessels, under the assumption that each vessel operates independently without mutual hydrodynamic interactions. For that reason Evans' conclusions are closely related to those found here.

higher-order modes correspond to flexural motions of polynomial form.

The capture width W corresponding to each of the first six Legendre polynomials is shown by the corresponding solid curve in Figure 11. A common feature is that for long wavelengths, W is proportional to the wavelength. This follows from the results noted at the end of Section 2 and from the fact that, if $\lambda/\ell \gg 1$, the vessel geometry is not significant. However, the magnitude and phase of each mode is optimized in these results, on the basis of (2.11), and for long wavelengths the corresponding values of (2.11) are unrealistically large. Indeed, it is readily shown in this case that $v_j = O(\lambda^{j+2})$ for large values of λ.

From the practical standpoint it is appropriate to limit the magnitude of the body motions, to be of the same order as the incident wave amplitude. Two pragmatic limits are shown by dashed lines in Figure 11. The relevant parameter here is the product of v_j and the beam-length ratio of the vessel. Representative values for this product have been chosen to correspond with typical values of the beam-length ratio for a slender wave-absorber of ship-like proportions.

The extraction of wave power from the rigid-body motions in pitch and heave requires an external force or moment acting on the vessel, and therefore a rigid foundation or mooring system. The higher-order modes of motion are attractive in so far as power can be extracted from the relative motion between different elements of the device, which is moored only against the second-order mean drift force of the waves. For this reason it is appropriate to impose the condition that the vessel is free to respond to the waves in heave and pitch, without an external first-order restraint.

As a consequence of the slender-body approximation, the latter condition is satisfied by the higher-order modes $n = 2,3,\ldots$, and more generally by any mode shape which is orthogonal to the Legendre polynomials $P_0 = 1$ and $P_1 = x$.

Trigonometric mode shapes tuned to the incident wavenumber can be expected to give better performance than a simple polynomial, expecially for shorter wavelengths. A suitable pair of even and odd modes orthogonal to heave and pitch are given by the expressions

$$f_e = \cos(kx) - j_0(k\ell/2), \tag{5.3}$$

$$f_o = \sin(kx) - (6x/\ell)j_1(k\ell/2), \tag{5.4}$$

14

Here $j_{0,1}$ are spherical Bessel functions of the first kind. The corresponding capture widths are shown in Figure 12. These results are similar to the Legendre function modes n = 2,3 for long wavelengths, but for short wavelengths the improved performance is apparent.

As an alternative to these continuous mode shapes we consider an articulated raft with rigid elements, joined by two symmetrically placed hinges. Two modes of motion are defined, orthogonal to heave and pitch, as depicted in Figure 13. The corresponding values of the capture width are shown in the same figure. Similar calculations indicate that the hinge position is not an important parameter, provided only that the hinges are not close to the ends of the raft. A raft with three elements of equal length appears to be most practical. It follows also that a raft with only one hinge at the center will perform with approximately the same performance as for the even mode shown in Figure 12, but without the added degree of freedom permitted by the corresponding odd mode. (When the two hinges approach the center, the odd mode shown in this figure tends to a discontinuous shearing motion at the center.)

Since the even and odd modes can be superposed, the total capture width in the above examples may approach a peak value close to the total length ℓ of the vessel. Since the continuous mode shapes shown in Figures 11 and 12 attain similar capture widths, it is likely that the articulated raft with two hinges is nearly optimum and no significant benefit will result from the number of hinges beyond this number.

With optimum tuning the even and odd modes of body motion are in quadrature. These combine to give a wavelike motion along the vessel with the phase velocity of the incident wave. The amplitude of this motion is symmetrical fore-and-aft, in agreement with the analogous finding of Evans (1979). This result differs from the conclusion in Section 4 based on a two-dimensional mode, where the optimum motion is concentrated primarily at the end facing the incident waves. This distinction can be attributed to three-dimensional diffraction, with the incident wave energy focused upon the after end of the body from the sides.

The performance in a spectrum can be computed as in (3.1) - (3.2). As an example we show in Figure 13 the total power extracted in a Pierson-Moscowitz spectrum by a raft with two hinges, as a function of the overall raft length.

15

The calculations of this section are based on the "ordinary" slender body approximation which assumes the beam and draft small compared not only to the length of the vessel, but also to the wavelength. A "unified" approximation has been developed to remove the latter restriction, as described by Mays (1978) and Newman (1978). Recent computations with this more refined approach indicate capture widths which are slightly less than those shown in Figure 12, but this reduction is at most 10%. Further work to improve upon the slender-body approximation will be reported in future publications.

6.   DISCUSSION AND CONCLUSIONS

Devices for absorbing wave energy can be categorized from the hydrodynamic viewpoint according to the following list:

(1) Floating or submerged
(2) Rigid or flexible elements
(3) Stationary or freely floating
(4) Two- or three-dimensional configuration
(5) Large device or point absorber

The first two characteristics in this list are of relatively little importance from the standpoint of wave-power absorption. This is suggested by the global analysis in Section 2, from which it follows that the optimum power absorption depends essentially on the ability of the vessel to radiate waves in a preferred direction. As in the analogous case of laboratory wavemakers, this property can be achieved with more-or-less equal success by a variety of devices which are floating or submerged, consisting of either rigid elements, pneumatic chambers, or other means for forcing oscillatory motion of the adjacent fluid.

A comparison of Figures 1 and 10 illustrates the similarity in optimum performance for two different types of device, the Salter cam and the two-dimensional Cockerell raft. Similar results may be anticipated for all two-dimensional devices. Indeed, any two-dimensional vessel with two or more suitable degrees of freedom and an optimal control system can operate with 100% efficiency!

More important is the question of whether the device is stationary

16

or freely floating. In this context "stationary" implies a fixed refer-
ence from which to exert an optimum restraining force on the device.
Most wave absorbing devices have been designed on this basis. Generally,
if they are freely floating, or fixed in mean position by a "slack" moor-
ing which exerts no first-order oscillatory force, the resulting perfor-
mance is degraded. Figure 3 illustrates this effect for the case of a
Salter cam. Large structures which are mounted on the ocean bottom in a
fixed manner should be included in the same category as stationary ves-
sels. By comparison, devices which extract power through the relative
motion between adjacent elements can be designed for efficient perform-
ance with a slack mooring system.

The fourth characteristic listed above is intended to place in a
separate category those devices which are based on a two-dimensional
analysis, and which therefore must be elongated in the direction parallel
to the wave crests. This two-dimensional configuration offers the obvi-
ous advantage of absorbing power uniformly along a broad expanse of the
incident wave front. In principle, 100% efficiency can be attained in
this manner, and the theoretical analysis associated with these devices
is relatively simple. On the other hand, two-dimensional configurations
must expose a large projected area to the incident waves, and therefore
experience proportionally large mooring forces.

Three-dimensional devices interact with the surrounding wave field
in a more complicated manner. Suitably designed, such devices have the
potential ability to absorb the wave energy over a capture width substan-
tially larger than the transverse projection of the device itself. This
desirable attribute follows from the nature of three-dimensional wave
diffraction, which is enhanced by the optimum interactions of different
elements of the vessel. Analogous effects result from the mutual inter-
action of several small vessels, in the manner described by Evans (1979).
Similar considerations are well known in the design of radio antennas
and phased sonar arrays.

The last of the hydrodynamic characteristics in the list above is
the size of the vessel in relation to the wavelength. Vessels which are
long can diffract the incoming waves in the manner described above,
while those which are wide can operate in a quasi-two-dimensional
manner. Intermediate between these are axisymmetric vessels, of inter-
est primarily in the context of small "point-absorbers" with horizontal
dimensions much less than the wavelength. The economy and operational

simplicity of such devices has been stressed especially in the work of Budal and Falnes. Point absorbers take advantage of three-dimensional diffraction to absorb the incident energy over a maximum capture width of half a wavelength, as noted in Section 2. (For heaving motion only, the maximum capture width is about one sixth of a wavelength.) Large amplitudes of motion are necessary to approach these maximum capture widths, and a stationary reference frame is required for the restraining force.

The most important hydrodynamic characteristics of a wave absorbing device are its size and configuration in relation to the incident wave field, and its requirement for a stationary reference position or alternatively a slack mooring. There are obvious practical and theoretical advantages associated with an elongated device, such as a slender Cockerell raft. The same considerations apply to other devices with a similar configuration, notably the Kaimei ship and the French air bag. With suitable optimization of their design, these elongated vessels are capable of performing at similar levels, with capture widths comparable to their lengths.

The computations in Section 5 are intended to illustrate the potential output from these types of vessels, for mode shapes of simple mathematical form defined by polynomials, trigonometric functions, and articulated elements. An ideal wave absorber would have a more complicated mode shape, chosen to maximize the capture width at each wavelength. The determination of this ideal mode shape has not been made, but it is reasonable to expect this to be a continuous wavelike motion along the body. The resulting power will exceed that from any of the simpler mode shapes illustrated in Section 5. An estimate of the ideal output can be inferred from Figure 15, which shows the total capture width of both the trigonometric and two-hinge modes, reproduced from Figures 12 and 13 for the case of limited amplitude ratio 0.2. The envelope of these two superposed curves is an indication of the maximum output obtainable in theory from an elongated flexible structure. It remains to be seen if a practical device can be developed which approaches this output.

ACKNOWLEDGEMENT

16

REFERENCES:

1. Evans, D.V. 1976. A theory of wave power absorption by oscillating bodies, *J. Fluid Mech.* 77, 1.

2. Evans, D.V. 1979. Some theoretical aspects of three-dimensional wave energy absorbers, *Symp. on Ocean Wave Energy Util.*, Gothenburg, Sweden.

3. Haren, P. & Mei, C.C. 1979. Wave power extraction by a train of rafts: hydrodynamic theory and optimum design, *Appl. Ocean Res.* 1, 147.

4. Hasselmann, K. et al. 1973. Measurement of wind wave growth and swell decay during the Joint North Sea Wave Project (JONSWAP), Deutches Hydrographische Institut, Hamburg.

5. Mays, J.H. 1978. Wave radiation and diffraction of a floating slender body, Ph.D. Thesis, Ocean Engineering, Mass. Inst. Tech., Cambridge, Mass., U.S.A.

6. Mei, C.C. 1976. Power extraction from water waves, *J. Ship Res.* 30, 63.

7. Mei, C.C. 1978. Numerical methods in water wave diffraction and radiation, *Ann. Rev. of Fluid Mech.* 10, 393.

8. Mynett, A., Serman, D.D. & Mei, C.C. 1979. Characteristics of Salter's cam for extracting energy from ocean waves, *Appl. Ocean Res.* 1, 13.

9. Newman, J.N. 1976. The interaction of stationary vessels with regular waves, *Proc. 10th Symp. Naval Hydro.*, London.

10. Newman, J.N. 1978. The theory of ship motions, *Adv. Appl. Mech.* 18, 221.

11. Newman, J.N. 1979. The absorption of wave energy by elongated bodies, to appear in *Appl. Ocean Res.*

12. Serman, D.D. & Mei, C.C. 1979. Note on Salter's energy absorber in random waves, to appear in *Ocean Engineering*.

13. Wehausen, J.V. 1971. The motion of floating bodies, *Ann. Rev. of Fluid Mech.* 3, 237.
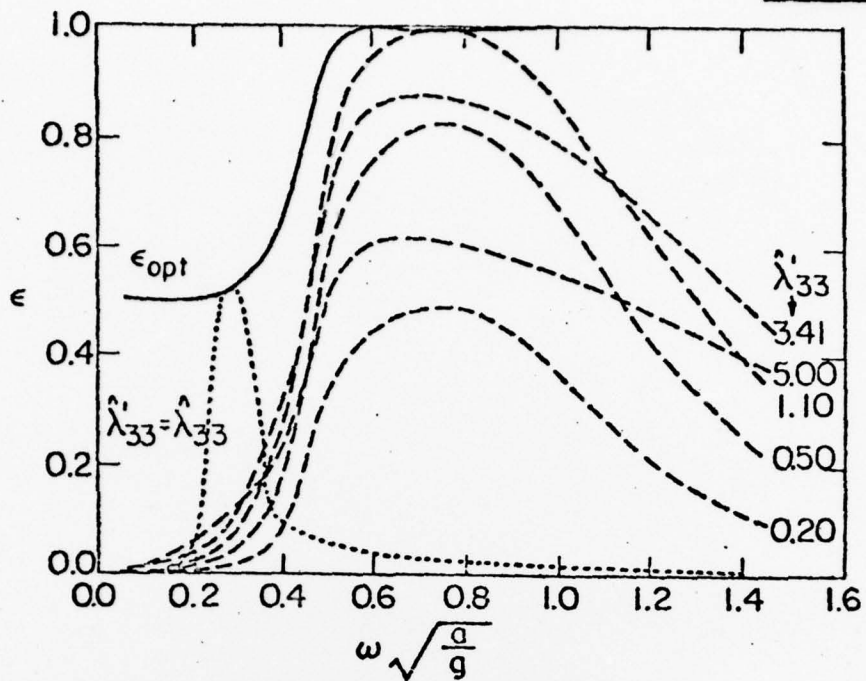
Figure 1: Efficiency of Salter's cam for varying frequencies and extraction rates. Unless otherwise noted each curve is for a fixed extraction rate $\hat{\lambda}'_3 = \hat{\lambda}'_{33}/\rho a^4\sqrt{g/a}$ and fixed inertia $I_3 = I_{33}/\rho a^4 = 1.9$. For the dotted curve (.....) $I_{33} = 13$, $\hat{\lambda}'_{33} = 0.4$.
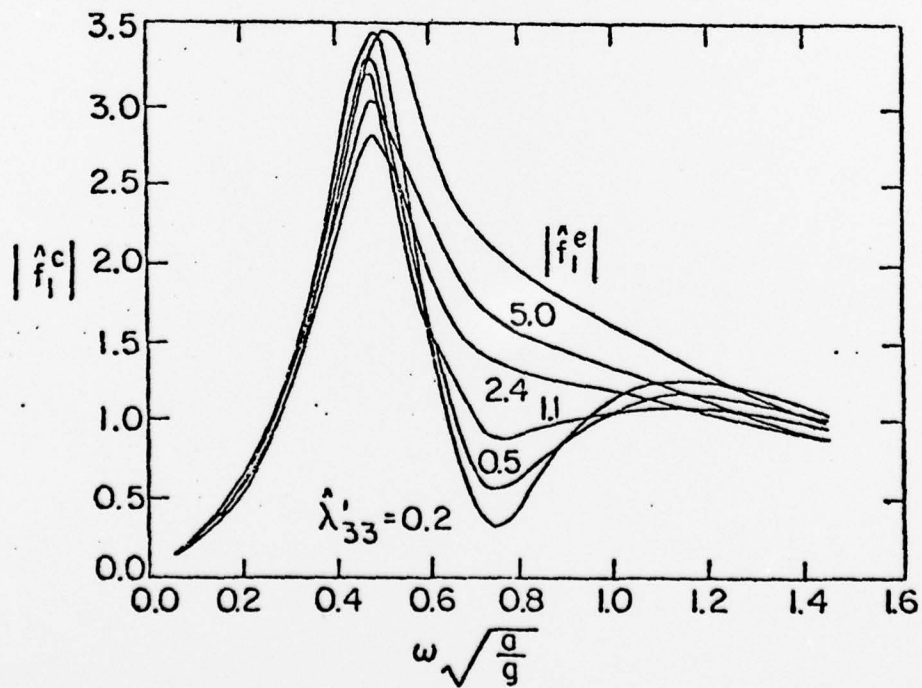
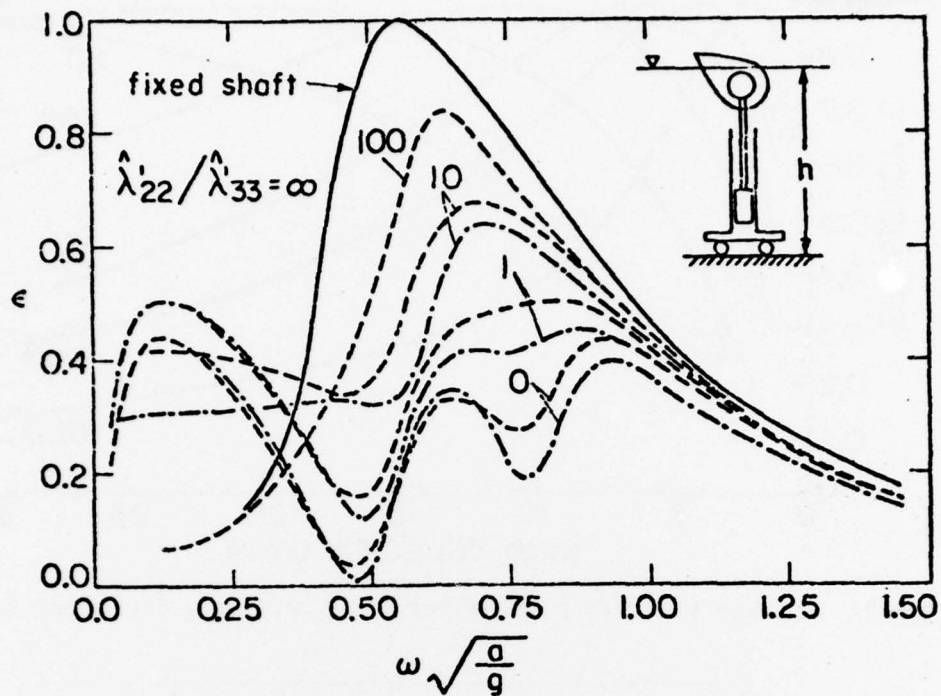**Figure 2:** Dimensionless horizontal wave force on the shaft $\hat{f}_1^c = f_1^c/\rho gaA$. The horizontal exciting force is also shown.

Figure 3: Efficiency of Salter's cam with three degrees of freedom. Energy can be extracted from the vertical motion, with various extraction rates $\hat{\lambda}'_{22}$.
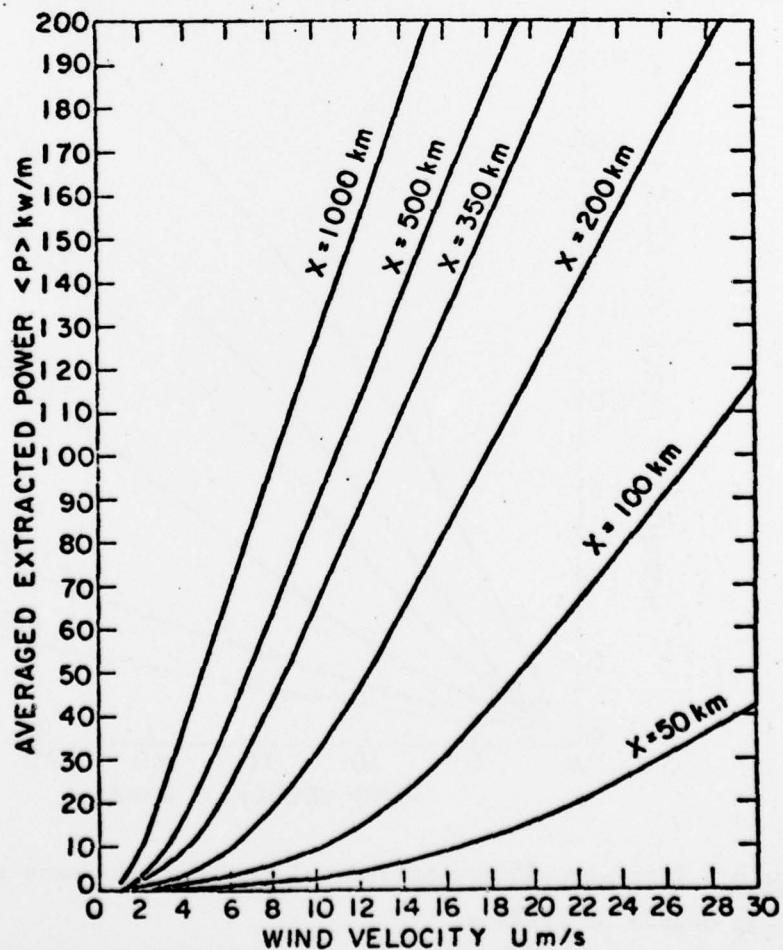
Figure 4: Average extracted power of Salter's cam with one degree of freedom. $a = 5$ m, $h = 20$ m. JONSWAP Spectrum.
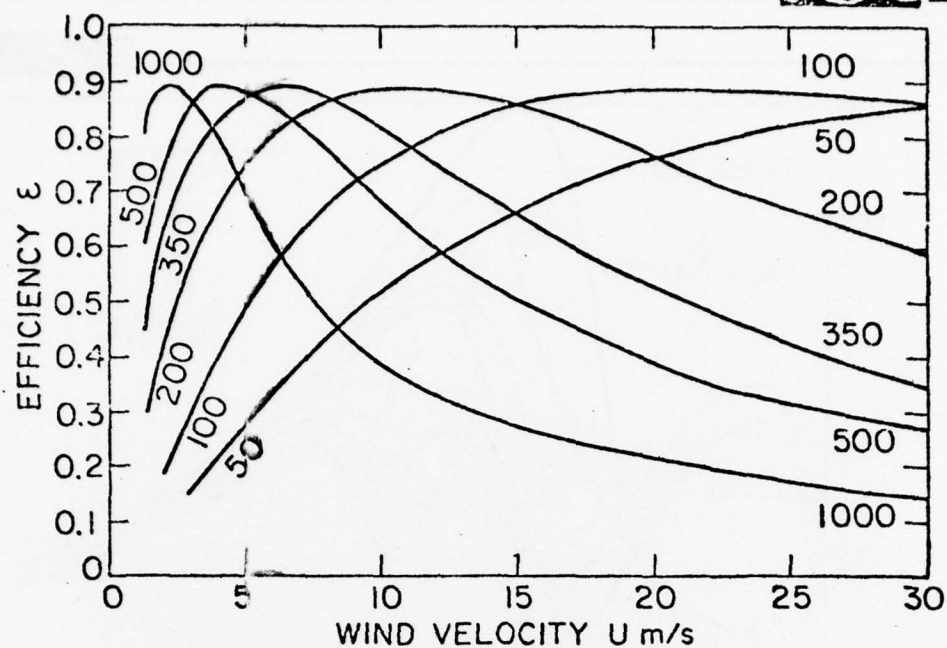
Figure 5: Average efficiency of Salter's cam with one degree of freedom.
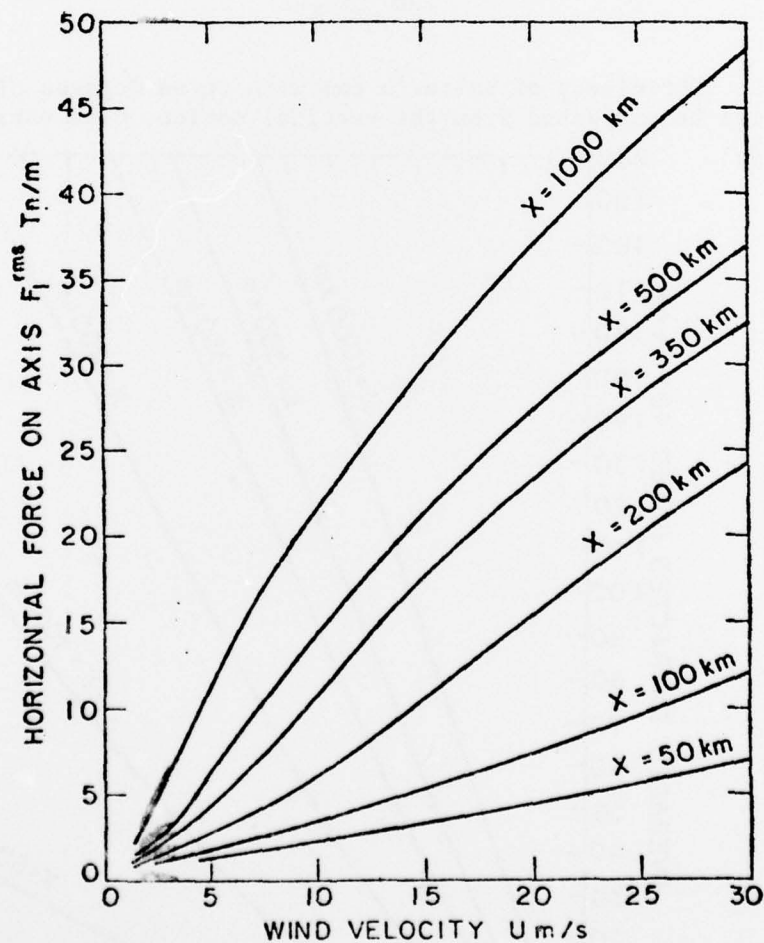
Figure 6: Root-mean-square horizontal force on the axis of Salter's cam with one degree of freedom.
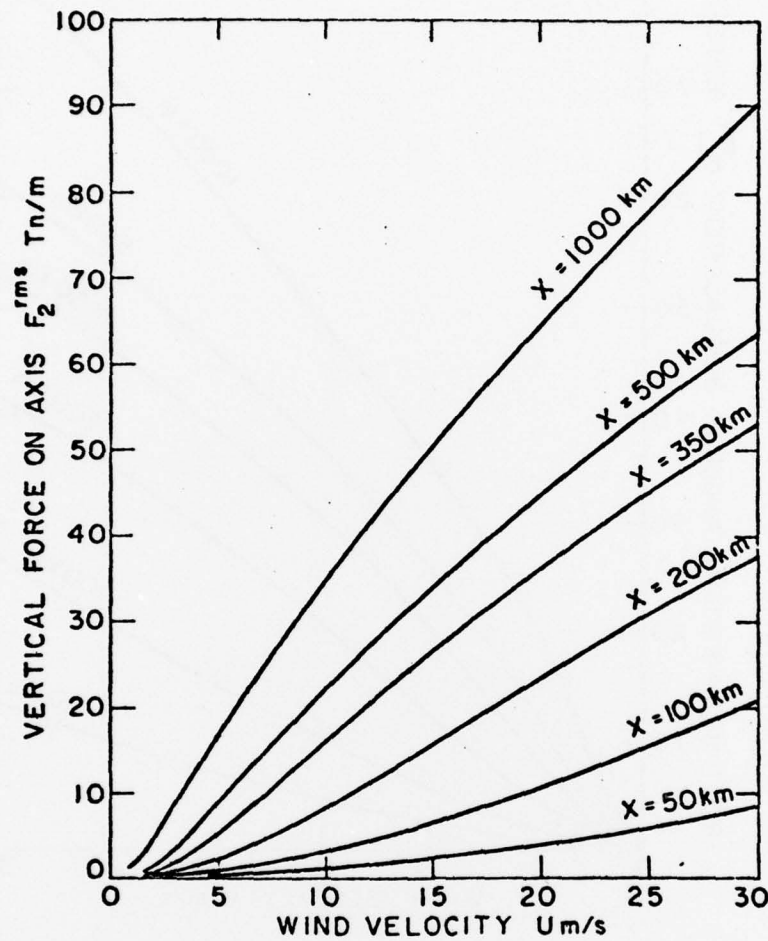
Figure 7: Root-mean-square vertical force on the axis of Salter's cam with one degree of freedom.
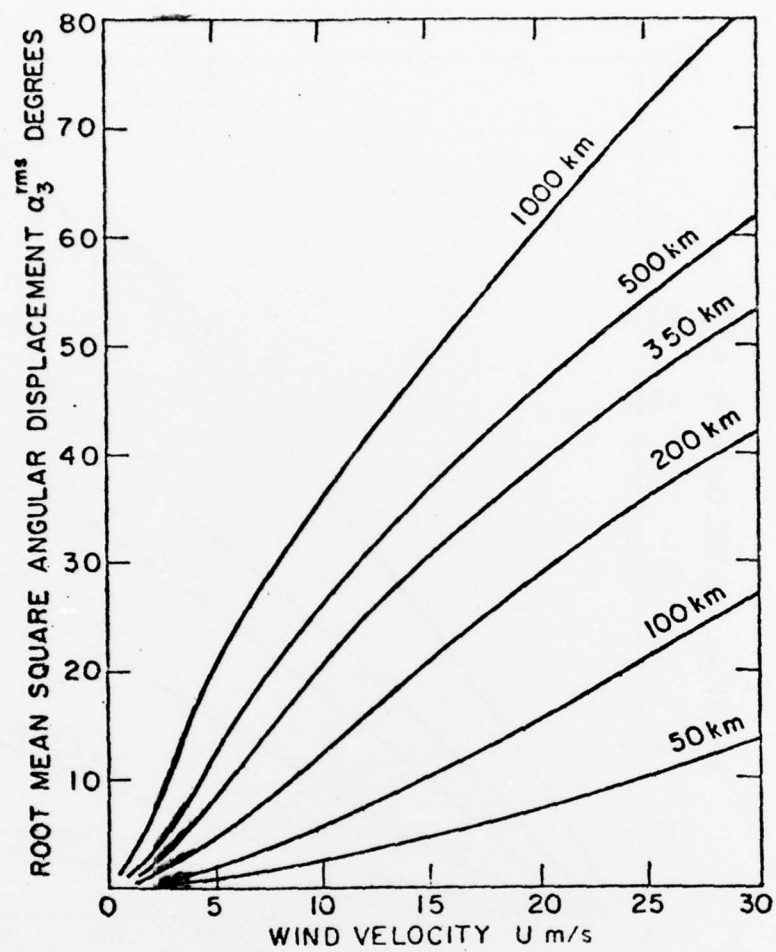
Figure 8: Root-mean-square angular displacement of Salter's cam.
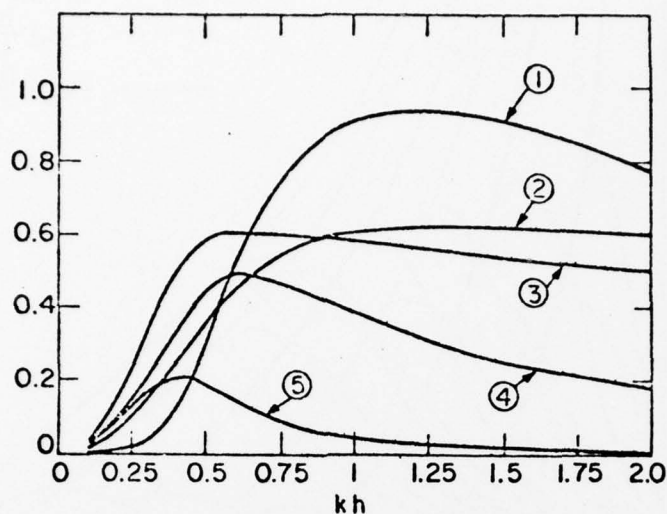
Figure 9: Properties of three raft train.

Curve (1): Fraction of extracted energy at the first hinge.

Curve (2) and (3): Vertical force at hinges 1 and 2, $f = F/\rho gAH$.

Curve (4) and (5): Relative rotation at hinges 1 and 2, $|\theta_2 - \theta_1| \times 10$ and $|\theta_3 - \theta_2| \times 10$ radians.
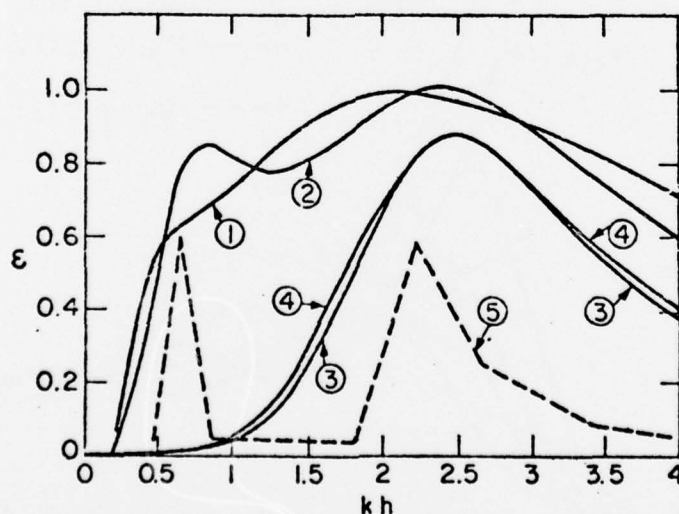
Figure 10: Efficiency of optimum designs for a double-peaked spectrum

Curves (1) and (2): Three and four raft trains for best averaged efficiency.

Curves (3) and (4): Three and four raft trains for best profit.

Curve (5): Spectrum (not to scale).
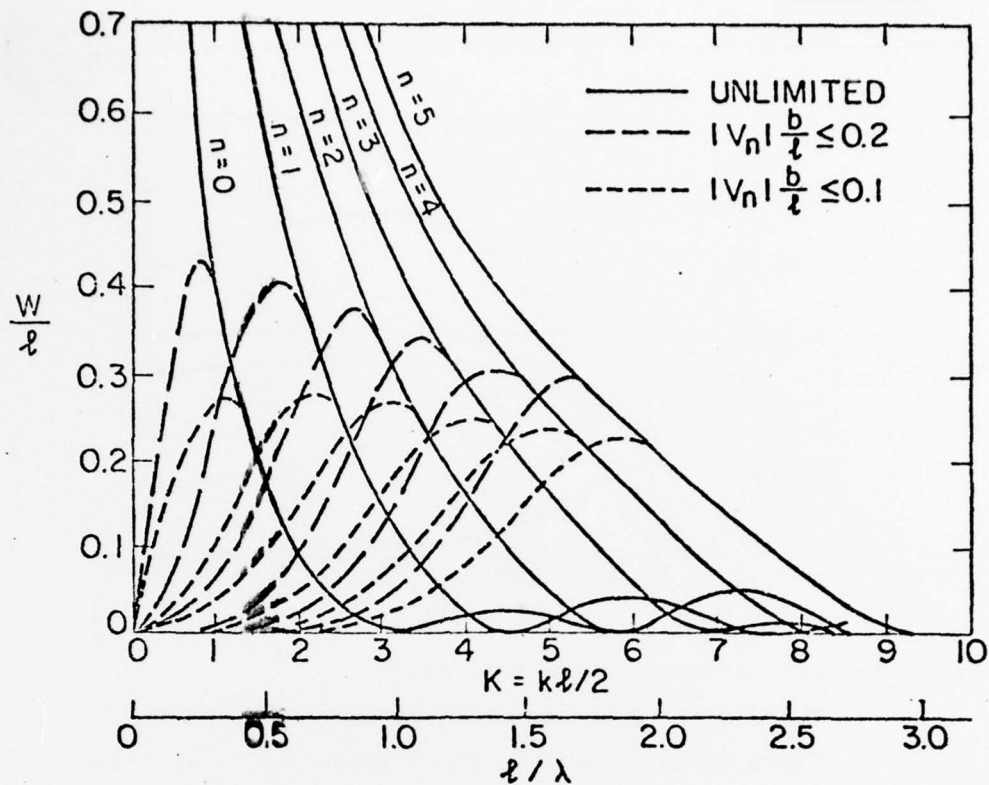
Figure 11: Absorption-width ratios W/ℓ, for Legendre polynomial modes of optimum magnitude and phase. The solid curves are for unlimited body displacement. The dashed curves correspond to arbitrary limits on the product of the body displacement amplitude $|v_n|$ and the beam-length ratio b/ℓ.
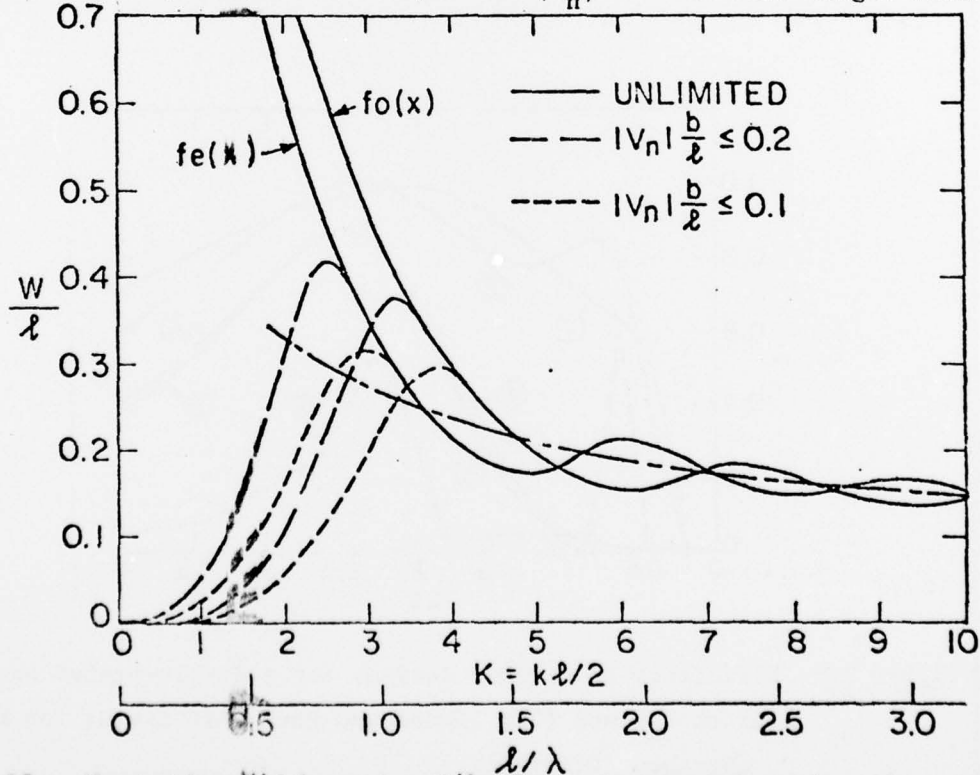

Figure 12: Absorption width ratios W/ℓ, for trigonometric modes of optimum magnitude and phase. Dashed curves are for the limited displacements defined in Figure 11. The asymptotic approximation for short wavelengths is superposed.
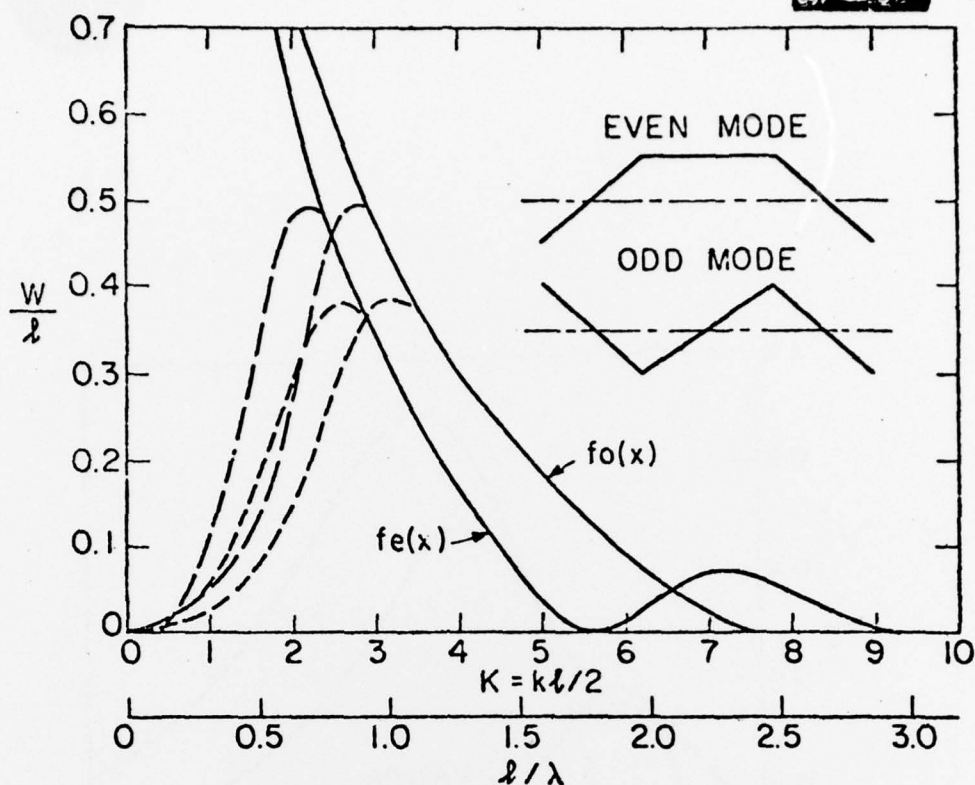
26

25

Figure 13: Absorption width ratios for a raft hinged at $x = \pm\ell/4$ with the modes of optimum magnitude and phase. Dashed curves are for the limited displacements defined in Figure 1.
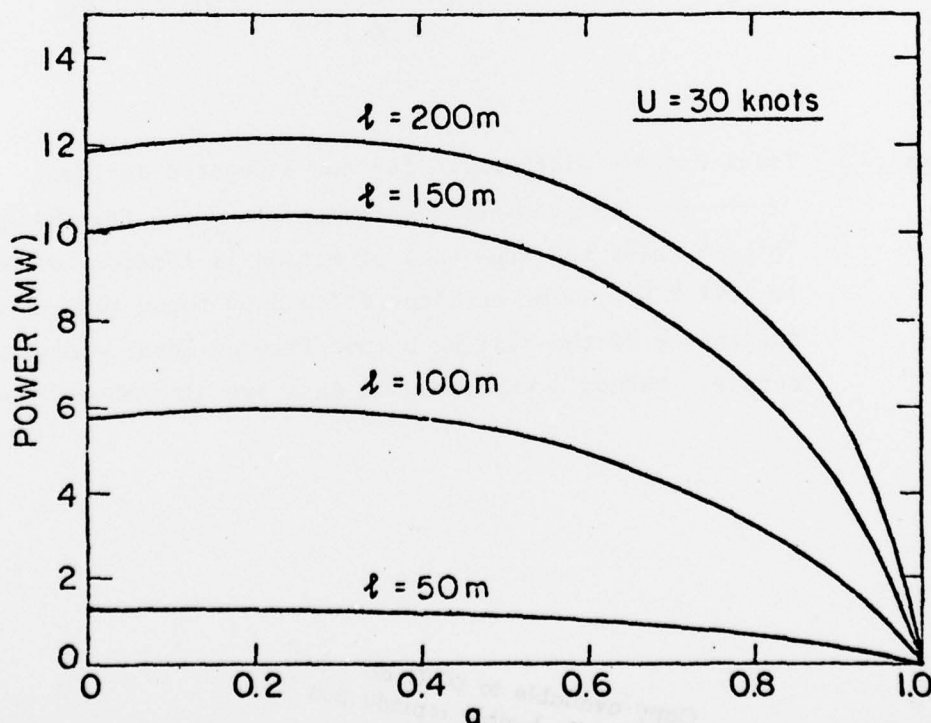

Figure 14: Performance of a hinged raft in the Pierson-Moskowitz spectrum corresponding to wind velocity of 30 knots

Other symbols are body length (ℓ) and hinge position (a) as a fraction of $\ell/2$. The maximum displacement is limited ($|v_n|b/\ell <$ 0.2), and optimum even and odd modes are superposed.
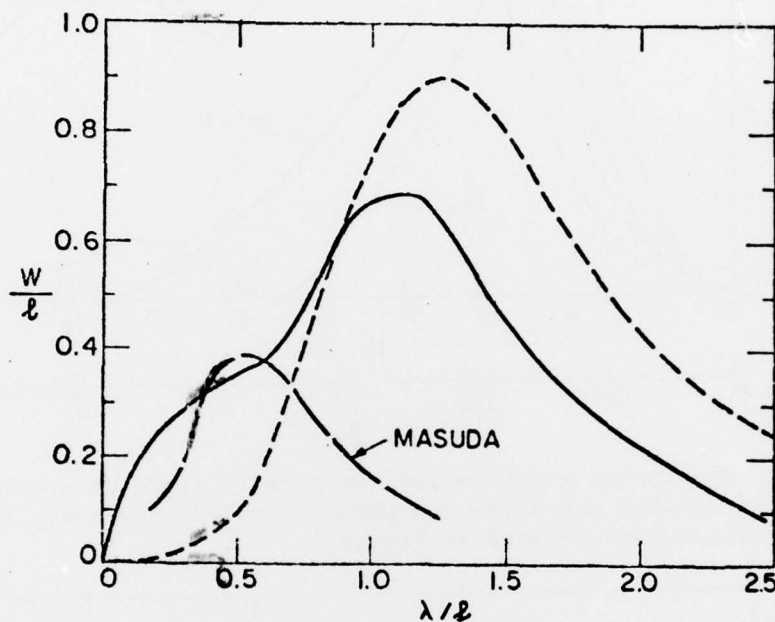
27

Figure 15: Total capture width ratio for two elongated devices:
———————— (trigonometric modes), ---------- (two-hinge raft).
In both cases the amplitude of motion is limited, with
$|v_n|b/\ell \le 0.2$. The envelope defined by these two curves is an
indication of the maximum output from an ideal elongated
device. Masuda's experimental data are also shown — — —.